

VisualCritic: Making LMMs Perceive Visual Quality Like Humans

Zhipeng Huang^{1,2*‡} Zhizheng Zhang^{2*‡} Yiting Lu¹ Zheng-Jun Zha¹
 Zhibo Chen¹ Baining Guo²

¹University of Science and Technology of China ²Microsoft Research Asia
 {hzp1104, luyt31415}@mail.ustc.edu.cn {zhazj, chenzhibo}@ustc.edu.cn
 zhizhangms@gmail.com bainguo@microsoft.com

Abstract. At present, large multimodal models (LMMs) have exhibited impressive generalization capabilities in understanding and generating visual signals. However, they currently still lack sufficient capability to perceive low-level visual quality akin to human perception. Can LMMs achieve this and show the same degree of generalization in this regard? If so, not only could the versatility of LMMs be further enhanced, but also the challenge of poor cross-dataset performance in the field of visual quality assessment could be addressed. In this paper, we explore this question and provide the answer "Yes!". As the result of this initial exploration, we present VisualCritic, the first LMM for broad-spectrum image subjective quality assessment. VisualCritic can be used across diverse data right out of box, without any requirements of dataset-specific adaptation operations like conventional specialist models. As an instruction-following LMM, VisualCritic enables new capabilities of (1) quantitatively measuring the perceptual quality of given images in terms of their Mean Opinion Score (MOS), noisiness, colorfulness, sharpness, and other numerical indicators, (2) qualitatively evaluating visual quality and providing explainable descriptions, (3) discerning whether a given image is AI-generated or photographic. Extensive experiments demonstrate the efficacy of VisualCritic by comparing it with other open-source LMMs and conventional specialist models over both AI-generated and photographic images.

1 Introduction

Research on Large Multimedia Models (LMMs) is at an exciting but still preliminary juncture. Current LMMs have shown impressive generalization capabilities in understanding high-level semantics [1, 22, 35, 70] and generating visual signals [17, 60, 61] in an instruction-following manner. Recent benchmark work [53] and our experiments have both found that current LMMs struggle to perceive the low-level quality of visual signals in line with human perception. To remedy

* Equal Contributions.

‡ This work was done when Zhipeng Huang was an intern at MSRA.

† Corresponding Author.

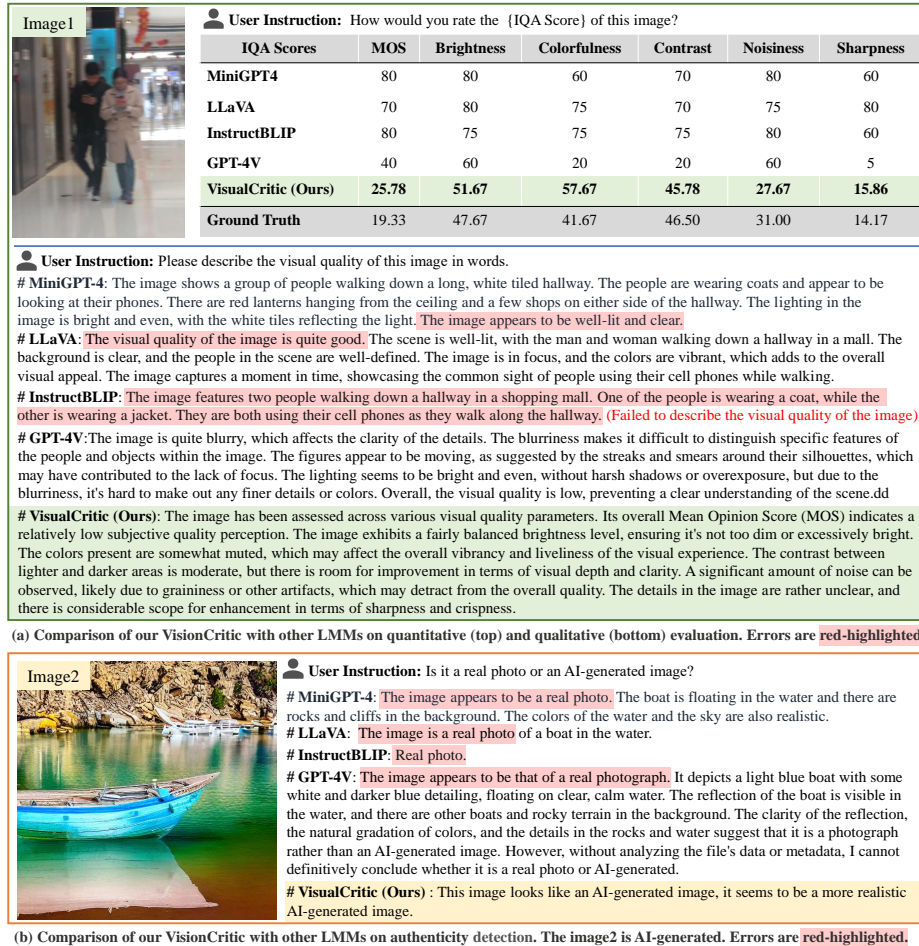


Fig. 1: Illustration of the comparison between existing LMMs and our proposed VisualCritic for visual subjective quality assessment from the perspectives of quantitative measurement, qualitative evaluation and authenticity detection. The results show VisualCritic is the best one of its kind to perform consistently well over different relevant tasks.

this shortcoming, we aim to comprehensively enhance the capability of LMMs in this aspect.

Visual quality assessment aims to qualify the perceptual quality of visual signals in accordance with human perception. In this field, conventional specialist methods [12, 43, 44, 49, 65, 68] have already achieved high statistical correlation with human subjective ratings for in-domain (within-dataset) settings. Although a given dataset can be well fitted, qualifying visual perceptual quality in a general scope remains highly challenging due to the diversity of visual signals and

the complexity of human perception. Amidst the vast volume and diversity of visual signals we experience daily, the broad applicability of this technology determines its genuine practicality. Besides, we believe in its potential immense value in interplaying with AIGC models for better visual alignment, by serving as a generic reward model. Just as an excellent cook typically necessitates a sensitive palate. Thus, constructing a generally applicable visual quality assessment model is indisputably important. Beyond numerical results, we also expect a generalist model for visual quality assessment to enable more functionalities, *e.g.*, explanatory descriptions or authenticity detection.

Nevertheless, both current LMMs and conventional specialist models are far from satisfactory in this aspect. Regarding the *generalizability*: The evaluation results in Figure 1 show that all LMMs, apart from ours, perform poorly in quantitative assessment, revealing clear gaps with humans ratings. Their basic quantitative assessment capabilities are lacking, let alone generalization. Conventional specialist models perform well for within-dataset visual quality assessment, but still struggle to cross-dataset evaluation due to unaligned human ratings over different datasets. They commonly rely on dataset-specific adaptation technologies [21, 26, 71], requiring access to the target domain thus limiting their practicality. Regarding the *versatility*: As illustrated in Figure 1, all open-source LMMs give the qualitative judgements obviously inconsistent with human perception. Their responses are more about semantic captions instead of the visual quality. GPT-4V [35] is able to give a basically reasonable response, but also tends to output semantic captions for scene understanding. All LMMs, apart from ours, fail to distinguish an AI-generated image. Conventional models do not supported these functionalities.

In this work, we make the first endeavour to build an LMM for broad-spectrum image subjective quality assessment, taking into account both generalizability and versatility. To this end, we find the model architecture is not the key, but an appropriate data construction and an effective training strategy are. We thus follow the common practices in building other LLMs [3, 7, 22, 25, 38, 70] to configure the model with a pre-trained vision encoder, a pre-trained LLM and a learnable adapter. Without a doubt, collecting a large-scale dataset with human ratings from scratch is extremely expensive. A straightforward solution is to combine publicly accessible datasets into a big one for joint training. However, in fact, this fails to deliver favorable results as we ever imagined, due to the rating inconsistency among different datasets. Detailed reasons are analyzed later. Through data analysis, we realize that the relativity of human ratings is much more transferable across different datasets than their absolute values. To utilize this characteristic, we propose a multi-stage curriculum learning strategy, in which we first perform the relativity learning on large-scale data from diverse sources and then adopt a few samples to unleash the capability of precisely estimating absolute scores. This effectively facilitates the learning of enabling an LMM to perceive low-level visual quality in a broad range akin to human perception.

As a result, we propose VisualCritic, the first LMM of its kind to support broad-spectrum image subjective quality assessment. Compared to conventional specialist models in the field of visual quality assessment, VisualCritic exhibits the state-of-the-art cross-dataset generalization ability over both photographic and AI-generated images. Besides, in addition to chat capabilities, it enables more domain-relevant functionalities for providing qualitative descriptions and performing authenticity detection.

2 Related Work

2.1 Large Multimodal Models

Recently, Large Multimodal Models (LMMs) have begun to showcase their preliminary prowess, riding on the coattails of the success of Large Language Models (LLMs). Initial research efforts [1,22,70] in this field have managed to accomplish preliminary multimodal universality by merely training a minimal number of parameters serving for adaptation and projection, effectively uniting frozen visual foundation models with pre-trained language foundation models. Subsequent research works further enhance their capabilities from different perspectives. Kosmos-2 [38], MiniGPT-v2 [3] and Ferret [59] enhance the spatial perception capabilities of multimodal large models, equipping them to be more applicable for a wide array of tasks with object bounding boxes involved. Kosmos-2.5 [30] develops the literate capability. Kosmos-G [36], MiniGPT-5 [69] and CM3Leon [61] try to unify both general-purpose semantic understanding and visual generation with a single model. Besides, there are a series of works building multimodal agents [13, 42, 45, 55, 66] to systematically complete their functionality and enhance their practicality in different application scenarios. In this work, we make the first endeavour towards a leap in the low-level perception capability of LMMs for visual quality.

2.2 Visual Quality Assessment

Visual quality assessment aims to quantify the perceptual quality of visual signals in accordance with human perception, beyond classic metrics like PSNR or SSIM [52]. Full-reference Image Quality Assessment (IQA) [12, 49] requires estimating the quality distance of the distorted image between the reference image to then estimate the quality score of the distorted one. In contrast, a more challenging and practical task setting is the no-reference image quality assessment [43, 44, 65, 68], also known as blind image quality assessment, wherein no reference images are provided. In this field, it is relatively easy to fit a given dataset while the real challenge lies in being generally applicable for samples in the wild. For this, cross-dataset adaptation technologies [21,26,71] are developed. But they require the annotations of target datasets for model fine-tuning, which limits their practicality and imposes strong application and research demands for developing an IQA generalist model that could be used out of the box on diverse data.

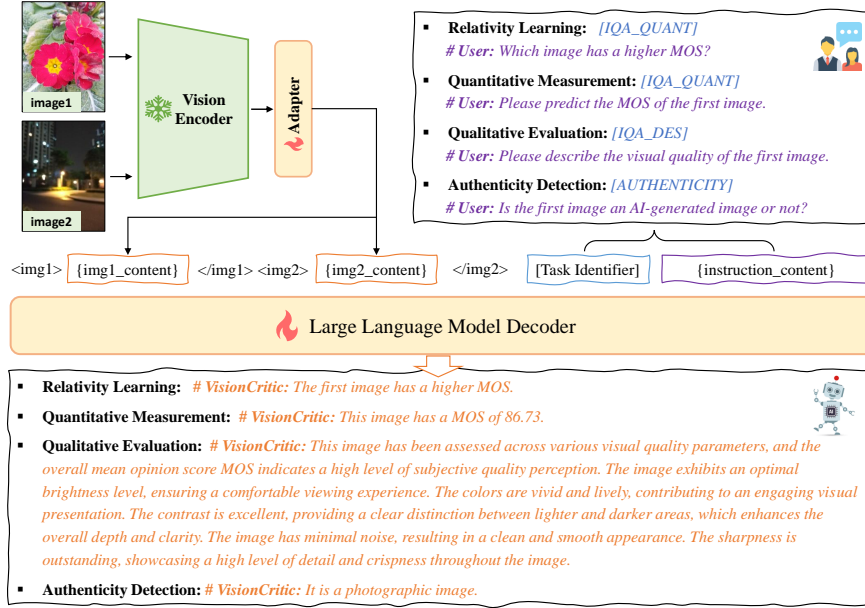


Fig. 2: The framework of our proposed VisualCritic, which comprises a frozen vision encoder, a learned cross-modality adapter and a LoRA-tuned LLM decoder. VisualCritic is the first of its kinds to support diverse visual quality assessment tasks, including relative quality comparison, quantitative measurement, qualitative evaluation and authenticity detection.

With the advent of large-scale models, GPT-4V [35] has been explored to evaluate text-to-image results from the perspective of design quality in [24] and shows very preliminary promise in predicting human preference for visual aesthetics and text-image alignment [54]. For IQA, as we evaluated, it can provide basically reasonable textual descriptions, but cannot accurately predict quantitative results or distinguish between AI-generated images and real images. Besides, a series of open-source LMMs are evaluated right out of the box in [53] but they all perform poorly on quantitative visual quality assessment. We are the first to construct an LMM for IQA with unprecedented generalizability and versatility. In addition to quantitative assessment as prior specialist models, our model can further provide linguistic descriptions and accomplish authenticity detection.

3 VisualCritic

3.1 Model Architecture

As indicated in recent reports [12, 49], current LMMs have preliminarily shown the potential to capture the perceptual quality of images, but they still cannot make precise judgments and support comprehensive assessment in the general scope. For our VisualCritic, we inherit as much world knowledge as possible and

the conversational ability from the pre-trained weights and infuse new knowledge to endow it with our target capability. As illustrated in Figure 2, VisualCritic consists of a vision encoder, a LLM decoder and a cross-modality adapter as common designs in [3, 22, 30, 38, 70]. In specific, we adopt a pre-trained EVA model [9] as the vision encoder to encode vision inputs into a series of tokens. These tokens are transformed to the input embedding space of a LLM decoder by an adapter with the same architecture as that in [22]. We adopt an open-sourced Vicuna-13B [6] as the LLM decoder. We empirically find the model architecture is not the key to VisualCritic, instead, the data construction and the training strategy are. We delineate them in the following.

3.2 Data Construction

Given an image x , VisualCritic could assess its perceptual quality by not only estimating a series of quantitative metrics y_{score} like conventional specialist models but also providing natural language descriptions y_{desc} . This advances explainable visual quality assessment. Besides, it can also distinguish whether a given image x is AI-generated or not, outputting y_{aigc} . We introduce their corresponding data construction respectively as follows.

Quantitative measurement. VisualCritic quantitatively assesses the perceptual quality of given images by estimating the most commonly used metric for subjective quality, *i.e.*, Mean Opinion Score (MOS) [46], and a series of quality attribute indicators including the brightness, colorfulness, contrast, noisiness, and sharpness. To enable this, we gather data with human subjective ratings from different public sources (details are listed in Table 1) and normalize the numerical annotations to the range of $[0, 100]$.

Nevertheless, training a visual quality assessment generalist with mixed datasets is much more challenging than we ever imagined. We experimentally find that straightforwardly combining samples from different datasets in joint training even performs worse than training on a single dataset when performing cross-dataset evaluation. This is because subjective annotations of different datasets are collected in different experiment environments and from different annotators [21]. Due to the inherent differences in visual quality among different datasets, it is difficult for different annotators to score a certain dataset with a unified standard over all datasets. **Such inconformity starves generalization.**

An intuitive way to address this inconformity issue is to rebuild a large-scale dataset over diverse images and have annotators score with a unified standard, which is, however, quite costly and hard to accomplish. Considering that the judgement of relative quality is obviously easier to generalize, we propose a curriculum learning scheme. Specifically, we first teach VisualCritic to discern the relativity of visual quality using large-scale data from diverse sources, then use a few samples without the label inconformity issue to enable it to further output absolute scores. We take MOS as an example to introduce the data construction process in detail, with other metrics employing analogous methods. For the relativity learning, we sample two different images $\{x_1, x_2\}$ from the

same dataset each time, and set the corresponding label $y_{mos} = [1, 0]$ if the MOS of x_1 is higher than that of x_2 , otherwise $y_{mos} = [0, 1]$. Then, we prompt GPT-4 [34] to generate the dialogue data upon the relative quality labels following the conversation template design of Vicuna [6]. For the absolute score estimation, we take the normalized MOS as its corresponding labels, and structure the training data in a dialogue form, following a shared format used for relativity learning. This unified format will be detailed in the following.

Qualitative evaluation. VisualCritic can further provide qualitative evaluation regarding the perceptual quality of given images in a more comprehensive view. The outputs incorporate but are not limited to various indicators in quantitative measurement, beyond their numerical values, enabling interpretability. To achieve this, given each sample, we prompt GPT-4 [34] to generate its corresponding dialogue-form training data in the same format with that for quantitative measurement on top of the ground truths of aforementioned quantitative indicators. The knowledge of GPT-4 is distilled in the annotations of our training data in this way. As a result, VisualCritic integrates the knowledge pertinent to visual quality assessment from its own pre-trained weights, GPT-4 and multiple public datasets, making it be a model “standing on the shoulders of giants”.

Authenticity detection. Aforementioned functionalities of quantitative measurement and qualitative evaluation can be applied for both AI-generated and photographic images. Towards further versatility, VisualCritic is also endowed with the authenticity detection capability, *i.e.*, discerning whether a given image is AI-generated or photographic. For a given image x , its label regarding the authenticity $y_{auth} = 1$ if x is a photographic image, otherwise $y_{auth} = 0$. (x, y_{auth}) is prompted to be a dialogue form, analogous to those for quantitative measurement and qualitative evaluation. Details are in the supplementary.

Unified format and data summary. The training data for above three functionalities adopt a unified format following the conversation template design of Vicuna [6] as below:

Human: $\langle img1 \rangle \{img1_content\} \langle /img1 \rangle (\langle img2 \rangle \{img2_content\} \langle /img2 \rangle)$ [Task Identifier] {instruction_content}
Assistant: {answer_content}

In this format, $\langle img \rangle$ and $\langle /img \rangle$ are special tokens marking the start and end of the token sequence of an image, respectively. $\{img_content\}$, $\{instruction_content\}$ and $\{answer_content\}$ are three placeholders of the tokens of input image, user instruction and VisualCritic’s response, respectively. The contents in the brackets are optional, only existing in the training data of the relativity learning, not in others. Inspired by [3], we treat the learning for aforementioned three functionalities as a multi-task problem and introduce a task identifier [Task Identifier] to reduce the ambiguity across different tasks. It is instantiated as $\langle IQA_QUANT \rangle$, $\langle IQA_DES \rangle$ and $\langle AUTHENTICITY \rangle$ for quantitative measurement, qualitative evaluation

Table 1: Details of the datasets used for different training stages. *Relativity Learning* refers to the learning of ranking two images according to their subjective quality. *Quant.* denotes the training for enabling VisualCritic to quantitatively score images. *Quali.* represents the training for enabling qualitative evaluation.

Purposes	Datasets	Stage-1	Stage-2	Stage-3
Relativity Learning	KonIQ-10k [14], SPAQ [8], FLIVE [58], LIVEC [11], CGIQA-6K [67], AGIQA-3k [20], KADID-10k [23]	✓	✓	✓
Quant. & Quali.	KonIQ-10k [14]		✓	✓
Authenticity Detection	KonIQ-10k [14], AIGCIQA-2023 [51]		✓	✓
Instruction Tuning	LLaVA-Instruction [25], CCSBU-Aligned [70]			✓

and authenticity detection, respectively. We summarize all adopted datasets for different purposes in Table 1, and detail their corresponding training strategies subsequently.

3.3 Training Strategy

To ensure both high generalization performance and versatility, we introduce a multi-stage training strategy for VisualCritic, with each stage serving its own purpose as shown in Table 1. Let us detail them below.

Stage-1: relativity learning. We first subject VisualCritic to the relativity learning with large-scale data from different sources for enabling it to rank the relative quality of multiple image diversely. This can effectively address the label inconformity issue on visual subjective quality across different datasets and is consistent with the intuition that it is easier to rank image of different quality than to rate them. In this stage, VisualCritic acquires preliminary perception for visual quality aligned with human preference.

Stage-2: multifunctional training. Afterwards, we perform multifunctional training to unleash the capabilities of quantitative measurement, qualitative evaluation and authenticity detection as introduced before. We integrate the data for different functionalities as described in Sec. 3.2 into a joint training framework, where we use $\langle \textit{Task Identifier} \rangle$ to differentiate tasks and each batch only contains one. In this stage, the knowledge of VisualCritic acquired in the stage-1 are further enhanced to accomplish specific tasks in an instruction following manner.

Stage-3: instruction tuning. Finally, we manually select some high-quality samples from the training data of the first two stages and combine them with general-purpose dialogue data to perform the instruction tuning for VisualCritic, so as to improving the quality and robustness of its responses to user instructions.

The data sources for the training of different stages are summarized in Table 1. They are all structured to be the aforementioned unified dialogue format in the way described in Sec. 3.2. This modelling allows us to train VisualCritic with a plain but universal auto-regressive optimization objective, which can be denoted

as below:

$$\text{maximize} \sum_{n=2}^{N_y} \mathbf{E}_{\hat{P}}[\log P(\mathbf{y}_n | \mathbf{x}_{1:N_x}, \mathbf{y}_{1:n-1})], \quad (1)$$

where $\mathbf{E}_{\hat{P}}[\cdot]$ is the expectation operator with respect to the distribution \hat{P} . Here, \hat{P} is the expected distribution (*i.e.*, ground-truth distribution) of P . $\mathbf{E}_{\hat{P}}[\cdot]$ is commonly implemented by a cross-entropy function between P and \hat{P} . $\mathbf{x}_{1:N_x}$ and $\mathbf{y}_{1:n-1}$ are the image tokens and preceding language tokens, respectively.

4 Experiments

4.1 Implementation Details

Throughout the training process, the visual backbone of VisualCritic remains frozen. The linear layer in the adapter and the language model are initialized with the weights of [70] and are trained efficiently with LoRA [15,32] techniques. We employ a rank setting of $r = 16$. The model is trained using a 224×224 image resolution at all stages. We employ the AdamW [29] optimizer paired with a cosine learning rate scheduler [28] for model training. In the first stage, we conduct training over 50,000 steps using $4 \times A100$ GPUs, with a global batch size of 96 and a base learning rate of $2e-4$. This stage is completed in approximately 12 hours. In the second stage, the model is trained for 10,000 steps on $4 \times A100$ GPUs, maintaining a global batch size of 96 and a base learning rate of $5e-5$, taking around 2 hours. Finally, the model undergoes an additional 5,000 training steps on $4 \times A100$ GPUs, with a global batch size of 64, completed in about 1 hour. The maximum learning rate remains constant at $1e-5$ during this final stage.

We normalize the ranges of human ratings with linear scaling to [0-100]. Note that the rating inconsistencies in specific values persist as analyzed in Sec. 3.2. This is the driving force behind our proposal of relativity learning.

Unless otherwise stated, we employ Spearman Rank Correlation Coefficient (SRCC) and Pearson’s Linear Correlation Coefficient (PLCC) as the evaluation metrics following the common practices in this field [43, 44, 53, 65]. More implementation details are provided in supplementary.

4.2 Quantitative Results

Comparison to LMMs. Our goal is to build an LMM that can perceive visual quality like humans. We thus first compare the proposed VisualCritic to other open-source LMMs in this aspect. The alignment between model outputs and human preference on the most widely used metric MOS is measured by two correlation coefficients SPCC and PLCC in Table 2. We can observe that across different datasets including both photographic and AI-generated ones, VisualCritic performs the best and outperforms other LLMs by a large margin.

Table 2: Comparison results (MOS) of our proposed VisualCritic with other LMMs on zero-shot visual subjective quality assessment. Metrics are shown as SPCC/PLCC. Ins-blip¹ is the abbreviation for InstructBLIP (Vicuna), and Ins-blip² stands for InstructBLIP (T5), the baseline of VisualCritic is MiniGPT4 [70]

Models	KonIQ-10k	SPAQ	FLIVE	LIVEC	CGIQA-6K	KADID-10k	AGIQA-3k
CLIP [39]	0.497/0.532	0.351/0.358	0.214/0.236	0.381/0.360	0.356/0.344	0.395/0.408	0.392/0.433
Llava-v1 [25]	0.494/0.500	0.426/0.459	0.258/0.290	0.363/0.391	0.054/0.088	0.374/0.401	0.601/0.669
Kosmos-2 [38]	0.280/0.305	0.653/0.649	0.204/0.204	0.377/0.380	0.207/0.215	0.358/0.368	0.516/0.506
InternLM [63]	0.587/0.635	0.738/0.753	0.359/0.413	0.573/0.649	0.176/0.172	0.533/0.567	0.711/ 0.772
Mplugowl [57]	0.476/0.482	0.645/0.650	0.236/0.273	0.367/0.403	0.094/0.103	0.473/0.495	0.666/0.698
Qwen-vl [2]	0.501/0.570	0.673/0.664	0.306/0.346	0.499/0.509	0.212/0.211	0.505/0.500	0.595/0.676
Shikra [4]	0.352/0.340	0.327/0.334	0.232/0.237	0.244/0.278	0.155/0.139	0.325/0.340	0.622/0.645
Llava-v1.5 [25]	0.471/0.487	0.547/0.575	0.304/0.337	0.372/0.438	0.306/0.313	0.417/0.432	0.625/0.748
Idefics [18]	0.405/0.434	0.468/0.488	0.234/0.243	0.411/0.438	0.179/0.201	0.368/0.383	0.551/0.614
Ins-blip ¹ [7]	0.383/0.458	0.688/0.689	0.189/0.268	0.206/0.330	0.198/0.230	0.343/0.387	0.611/0.665
Ins-blip ² [7]	0.312/0.307	0.602/0.632	0.219/0.220	0.000/0.039	0.066/0.110	0.281/0.240	0.235/0.255
Otter-vl [19]	0.421/0.424	0.478/0.484	0.140/0.139	-0.020/0.030	0.336/0.363	0.568/0.587	0.429/0.460
baseline [70]	0.276/0.289	0.250/0.275	0.180/0.199	0.315/0.314	0.224/0.199	0.248/0.246	0.572/0.584
VisualCritic	0.856/0.867	0.844/0.852	0.553/0.633	0.738/0.778	0.442/0.473	0.681/0.701	0.734/0.712

This demonstrates that our VisualCritic statistically achieves the highest consistency with human preference of visual perceptual quality among existing LMMs, whether for photographic or AI-generated images. It showcases a high potential for improved visual alignment. We selected the MiniGPT4 [70] as our baseline due to its straightforward implementation, allowing us to eliminate the confounding effects of more elaborate designs on our experimental results. A comparison of it with other LLMs is presented in Table 2. Moreover, it is impractical to require LLMs in Table 2 to be compared using the same training data since their pre-training and training are performed on large-scale general-purpose datasets. These datasets may already encompass the data for IQA. Additionally, the data construction is a key factor in determining the varying capabilities of different large models, which also stands as one of our main contributions.

We admit that there is still a performance gap between VisualCritic and SOTA IQA specialist models in terms of the within-dataset quantitative performance. Detailed comparison results can be found in our supplementary. The significance of developing VisualCritic, such an LMM for this lies in its generalizability and practicality. VisualCritic attains the performance over different datasets listed in Table 2 with a single model right out of the box, while a model is trained for a specific dataset for conventional IQA methods. The latter kind fits a given dataset well but suffers from poor cross-dataset generalization, severely limiting the practicality. To the best of our knowledge, VisualCritic is the first one of its kind to handle such diverse datasets including both photographic and AI-generated samples simultaneously. It can be constructed upon a commonly used LMM architecture, trained with a plain auto-regressive loss and can be used effortlessly right out of the box without additional adaptation. Besides, VisualCritic provides rich functionalities as introduced before and has the chat ability.

Table 3: Comparison results (MOS) of our VisualCritic with conventional specialist models on the generalizable visual subjective quality assessment. The “*S*” and “*T*” denotes the source and target datasets, respectively. For *VisualCritic-S*, we only perform the training of Stage-2 and Stage-3, corresponding to a single-source generalization. For *VisualCritic-M*, we perform the training of all three stages with the target dataset discarded from the training data in all stages, corresponding to a multi-source generalization. Metrics are shown as SPCC/PLCC.

Models \ S→T	KonIQ-10k→KADID-10k→	LIVEC→	KADID-10k→	
	KADID-10k	KonIQ-10k	KADID-10k	LIVEC
DBCNN [64]	0.455/0.464	0.413/0.421	0.419/0.419	0.266/0.290
HyperIQA [47]	0.511/0.516	0.545/0.556	0.378/0.439	0.490/0.487
RankIQA [27]	0.487/0.426	0.603/0.551	0.416/0.390	0.491/0.495
MUSIQ [16]	0.486/0.504	0.554/0.573	0.497/0.524	0.517/0.524
GraphIQA [48]	0.521/0.536	0.427/0.430	0.365/0.393	0.388/0.407
CLIP-IQA [50]	0.655/0.655	-	-	-
VCRNet [37]	0.504/0.517	0.566/0.585	0.340/0.416	0.520/0.530
UCDA [10]	0.430/0.437	0.638/0.636	0.383/0.432	0.499/0.484
RankDA [5]	0.403/0.413	0.496/0.501	0.420/0.485	0.583/0.619
VisualCritic-S	0.656/0.668	0.657/0.676	0.559/0.533	0.645/0.646
VisualCritic-M	0.679/0.683	0.665/0.686	0.562/0.571	0.661/0.671

Table 4: Quantitative results on other indicators. For brightness, colorfulness, contrast, noisiness and sharpness, we report their corresponding SPCC/PLCC on the SPAQ [8] dataset that provides the ground truths for these indicators. For authenticity detection, we report the accuracy on the photographic dataset SPAQ [8] and the AI-generated dataset AIGCIQA-2023 [51].

Brightness	Colorfulness	Contrast	Noisiness	Sharpness	Authenticity
0.730/0.783	0.707/0.719	0.709/0.717	0.813/0.807	0.828/0.811	70.3%

Comparison to conventional IQA models. We further compare our VisualCritic with conventional IQA specialist models in terms of their cross-dataset generalization ability. Detailed results are in Table 3. For single-source generalization, *VisualCritic-S* is superior to conventional IQA models thanks to the integration of world knowledge from pre-trained weights (via parameter inheritance) and GPT-4 (via annotation refinement/generation). Regarding multi-source generalization, the proposed *VisualCritic-M* performs better on the target datasets, attaining 0.024/0.028, 0.062/0.050, 0.065/0.047, 0.078/0.052 improvements for the *KonIQ-10k*→*KADID-10k*, *KADID-10k*→*KonIQ-10k*, *LIVEC*→*KADID-10k*, *KADID-10k*→*LIVEC* settings on SRCC and PLCC, respectively, relative to the second best conventional IQA models. Compared to *VisualCritic-S*, the larger improvements achieved by *VisualCritic-M* demonstrate the effectiveness of our adopted relativity learning on the joint utilization of different IQA datasets.

Quantitative results on other indicators. Besides the most commonly used indicator, *i.e.*, MOS, we also report the quantitative results of our VisualCritic on other indicators in Table 4 to show its achieved versatility. Few publications report their performance on these indicators.

Table 5: Comparison results (MOS) of different training strategies for building VisualCritic. *MultiFunc_{joint}* refers to performing multifunctional training jointly over multiple datasets. *MultiFunc_{single}* refers to performing multifunctional training on a single dataset. (Here, we use KonIQ-10k.) *Relat.* is short for “Relativity Learning” for learning to rank multiple images according to their subjective quality. For all models in this table, the stage-3 training (instruction tuning) has been conducted, which is omitted for brevity. Metrics are shown as SPCC/PLCC

Methods	Datasets						
	KonIQ-10k	SPAQ	FLIVE	LIVEC	CGIQA-6K	KADID-10k	AGIQA-3k
<i>MultiFunc_{joint}</i>	0.621/0.664	0.701/0.703	0.247/0.197	0.476/0.485	0.130/0.141	0.337/0.263	0.477/0.484
<i>MultiFunc_{single}</i>	0.787/0.803	0.771/0.782	0.373/0.423	0.652/0.658	0.385/0.377	0.626/0.641	0.663/0.644
Relat. + <i>MultiFunc_{joint}</i>	0.643/0.682	0.726/0.716	0.251/0.203	0.479/0.513	0.171/0.183	0.384/0.333	0.525/0.537
Relat. + <i>MultiFunc_{single}</i>	0.856/0.867	0.844/0.852	0.553/0.633	0.738/0.778	0.442/0.473	0.681/0.701	0.734/0.712

Table 6: Comparison results (MOS) of different dataset choices for the training of quantitative measurement in Stage-2 (multifunctional training). The datasets used for the training of Stage-1 and Stage-3 remain the same as reported in Table 1. Metrics are shown as SPCC/PLCC

Source	Target	KonIQ-10k	SPAQ	FLIVE	LIVEC	CGIQA-6K	KADID-10k	AGIQA-3k
KonIQ-10k [14]		0.856/0.867	0.834/0.849	0.551/0.634	0.735/0.775	0.458/0.473	0.706/0.709	0.739/0.736
SPAQ [8]		0.731/0.762	0.865/0.864	0.487/0.511	0.718/0.716	0.387/0.406	0.502/0.536	0.721/0.700
FLIVE [58]		0.707/0.717	0.857/0.853	0.633/0.667	0.754/0.809	0.252/0.295	0.521/0.558	0.639/0.625
LIVEC [11]		0.760/0.747	0.807/0.822	0.582/0.580	0.857/0.864	0.399/0.398	0.578/0.591	0.645/0.684
CGIQA-6K [67]		0.525/0.535	0.689/0.718	0.467/0.465	0.526/0.540	0.710/0.725	0.398/0.384	0.630/0.656
KADID-10k [23]		0.677/0.703	0.748/0.760	0.472/0.488	0.682/0.713	0.425/0.462	0.855/0.843	0.747/0.713
AGIQA-3k [20]		0.602/0.585	0.638/0.662	0.440/0.419	0.573/0.577	0.211/0.223	0.416/0.442	0.846/0.806

Ablation study on the training strategy. We conduct an ablation study on the proposed training strategy for VisualCritic, with the results presented in Table 5. In this table, *MultiFunc_{joint}* corresponds to the straightforward way to build VisualCritic with a joint learning over different datasets. Nevertheless, it performs worse than *MultiFunc_{single}* that is only trained on a single dataset, in terms of both within-dataset (on KonIQ-10k) or cross-dataset (on other datasets) quantitative performance. This observation experimentally reveals the inconformity issue in this field and indicates that “the inconformity starves generalization” as analyzed in Sec. 3.2. Moreover, we observe that the model *Relat. + MultiFunc_{joint}* delivers clear improvements compared to the model *MultiFunc_{joint}*, and the same goes for comparing *Relat. + MultiFunc_{single}* to *MultiFunc_{single}*. This experimental observation demonstrates the effectiveness of our applied relativity learning on utilizing diverse datasets with unaligned annotations in building an IQA generalist. In specific, converting the absolute scores in each dataset into the judgements of relative quality can effectively make the model training free of the effects of the inconsistency in the original annotations of different datasets. Furthermore, the model *Relat. + MultiFunc_{single}* performs the best across all model variants, demonstrating the superiority of our proposed training strategy for VisualCritic. This experimental phenomenon

provides an insight that the annotation inconsistency over different datasets inevitably affects the results of multifunctional training (Stage-2) as well. In the following, we study the effects of choosing different datasets when performing multifunctional training on the final results.

Ablation study on the dataset choice. Actually, in Table 2, only the performance on the KonIQ-10k dataset could not be affected much by the annotation inconformity issue across different datasets. For other datasets except KonIQ-10k, we only utilize the relativity of their data annotations for the Stage-1 training, without using their absolute numerical values. Therefore, the performance on these datasets could be considered to reflect a certain degree of generalization. Here, we zoom into the effects of the dataset choice used for the training of quantitative measurement in the Stage-2, denoted by the ‘‘Source’’ in the Table 6. As the results show in Table 6, for each test dataset denoted by ‘‘Target’’, the highest performance is reached when its corresponding training set is used for the training of quantitative measurement in the Stage-2. We find the data configuration in Table 1 achieves the best trade-off between different datasets when tackling the aforementioned annotation inconformity issue. Additionally, partially combining some of them for a joint training, instead of using them all, for *MultiFunc_{joint}* in Table 5 is not the research focus of this work, we provide some results in the supplementary.

Table 7: Human side-by-side comparison of ours with other LLMs in qualitative Results.

G+S/S+B	GPT-4V [35]	LLaVA-v1.5 [25]	MiniGPT-4-13B [70]	InstructBLIP [7]
VisualCritic (Ours) v.s.	1.29	1.77	1.82	2.45

4.3 Qualitative Results

We show the qualitative results in Figure 1. From this case study, we can find that our proposed VisualCritic exhibits impressive instruction following capability with more detailed and pertinent descriptions compared to other LMMs, when being asked to assess the visual quality of the given image. In addition, other LMMs all misjudge the given AI-generated image as a photographic one while our VisualCritic makes the correct judgment. Besides these performances, VisualCritic also minimizes the generation of hallucinations and actively admits its unknown or uncertain judgments. More related qualitative results and their corresponding analysis are placed in our supplementary.

Quantitative evaluation of the linguistic outputs of LMMs remains an under-resolved issue so far. The common compromise solution is to employ a more advanced LMM (*e.g.*, GPT-4V) as a critic for evaluating other models. But this is not adaptable to this work since our proposed model is at the forefront in this field. To address this issue as possible, we conduct a human side-by-side evaluation where 10 users are employed for comparing ours with 4 other LMMs on 100 random samples. The G+S/S+B scores (where **G**ood: our VisualCritic

<p>For Relativity Learning: You are an AI data construction assistant. I will give you the MOS values of two images. You need compare them and use natural language to tell me the comparison results. Your responses don't need to include any specific values. Example 1: ----- Input: ----- MOS of image1: 48.86 MOS of image2: 75.57 Output: ----- The latter image has superior quality. ----- Example 2: ----- Input: ----- MOS of image1: 63.64 MOS of image2: 37.55 Output: ----- The first image has superior quality. -----</p>	<p>For Quantitative Measurement: You are an AI data construction assistant. I will provide you a numerical indicator related to the visual quality of an image. Please insert this numerical indicator into a natural language description and return it to me. Example 1: ----- Input: ----- MOS: 48.86 Output: ----- The MOS score of this image is 48.86. ----- Example 2: ----- Input: ----- MOS: 76.33 Output: ----- For this image, the MOS score is 76.33. -----</p>	<p>For Qualitative Evaluation: You are an AI data construction assistant. Given some visual quality metrics of an image, you need return a linguistic description in terms of its subjective quality without mentioning specific values or file names. The metrics contains MOS (Mean Opinion Score), Brightness, Colorfulness, Contrast, Noisiness, and Sharpness, each ranging from 0 to 100. The higher the better. Example 1: ----- Input: ----- MOS: 48.86 Brightness: 48.86 Colorfulness: 47.43 Contrast: 55.57 Sharpness: 42.57 Output: ----- The image has been evaluated across various visual quality parameters. Its overall Mean Opinion Score (MOS) suggests a moderately good subjective quality perception. The image displays a balanced brightness level, ensuring it's neither too dim nor overly bright. The colors present are moderately vibrant, adding a touch of liveliness to the visual experience. There's a good distinction between the lighter and darker areas, enhancing the visual depth and clarity. The details are reasonably clear, though there might be room for improvement in terms of crispness. -----</p>	<p>For Authenticity Detection: You are AI data construction assistant. Given the authenticity score of an image, you need return a linguistic description in terms of its authenticity without mentioning specific numerical values or file names. This score ranges from 0 to 100. The higher the better. The image with an authenticity score lower than 100 should be considered as an AI-generated one, while those with a score of 100 are photographic/real images. Example 1: ----- Input: ----- Authenticity: 30.34 Output: ----- It looks very much like an AI-created image ----- Example 2: ----- Input: ----- Authenticity: 73.14 Output: ----- It looks very much like an extremely realistic AI-generated image. -----</p>
--	--	---	---

Fig. 3: LLM prompts for data construction. These prompts from left to right are for generating VisualCritic’s response (*i.e.*, $\{answer_content\}$) in the training data of relativity learning, quantitative measurement, qualitative evaluation and authenticity detection, respectively.

preferred, **Same**: no preference, **Bad**: other model preferred) are as shown in Table 7.

4.4 Prompts for Data Construction

As introduced in Sec. 3.2, we prompt GPT-4 to automatically construct training data from public datasets with human subjective ratings, avoiding substantial manual annotation costs. The training data adopt a unified format as introduced in Sec. 3.2, where $\{img_content\}$, $\{instruction_content\}$ and $\{answer_content\}$ are three placeholders of the tokens of input image, user instruction and VisualCritic’s response, respectively. The prompts to generate VisualCritic’s response (*i.e.*, $\{answer_content\}$) are illustrated in Figure 3 which are categorized into four segments, each corresponding to different image assessment functionalities task we investigate in Sec. 3.2. In the supplementary, we provide additional prompts tailored for generating user instruction (*i.e.*, $\{instruction_content\}$).

5 Conclusion

In this work, we explore the question: *Can LMMs perceive low-level visual quality aligned with human perception and show their excellent generalization ability in this regard?* We provide an answer with VisualCritic, the first LMM of its kind for broad-spectrum image subjective quality assessment. Compared to

conventional specialist models in the field of visual quality assessment, VisualCritic exhibits unprecedented cross-dataset generalizability and versatility. Beyond numerical scores, VisualCritic can further provide qualitative descriptions about visual quality and perform authenticity detection. We pinpoint the key to VisualCritic and introduce the core strategies on data construction and model training for making it real. We leave its extension to more data like videos and more functionalities in the future exploration. We also look forward to exploring its interplay with AIGC models for achieving better visual alignment.

References

1. Alayrac, J.B., Donahue, J., Luc, P., Miech, A., Barr, I., Hasson, Y., Lenc, K., Mensch, A., Millican, K., Reynolds, M., et al.: Flamingo: a visual language model for few-shot learning. *Advances in Neural Information Processing Systems* **35**, 23716–23736 (2022)
2. Bai, J., Bai, S., Yang, S., Wang, S., Tan, S., Wang, P., Lin, J., Zhou, C., Zhou, J.: Qwen-vl: A frontier large vision-language model with versatile abilities. *arXiv preprint arXiv:2308.12966* (2023)
3. Chen, J., Li, D.Z.X.S.X., Zhang, Z.L.P., Xiong, R.K.V.C.Y., Elhoseiny, M.: Minigt-v2: Large language model as a unified interface for vision-language multi-task learning. *arXiv preprint arXiv:2310.09478* (2023)
4. Chen, K., Zhang, Z., Zeng, W., Zhang, R., Zhu, F., Zhao, R.: Shikra: Unleashing multimodal llm’s referential dialogue magic. *arXiv preprint arXiv:2306.15195* (2023)
5. Chen, P., Li, L., Wu, J., Dong, W., Shi, G.: Unsupervised curriculum domain adaptation for no-reference video quality assessment. In: *ICCV* (2021)
6. Chiang, W.L., Li, Z., Lin, Z., Sheng, Y., Wu, Z., Zhang, H., Zheng, L., Zhuang, S., Zhuang, Y., Gonzalez, J.E., et al.: Vicuna: An open-source chatbot impressing gpt-4 with 90%* chatgpt quality. See <https://vicuna.lmsys.org> (accessed 14 April 2023) (2023)
7. Dai, W., Li, J., Li, D., Tiong, A.M.H., Zhao, J., Wang, W., Li, B., Fung, P., Hoi, S.: Instructblip: Towards general-purpose vision-language models with instruction tuning (2023)
8. Fang, Y., Zhu, H., Zeng, Y., Ma, K., Wang, Z.: Perceptual quality assessment of smartphone photography. In: *Proceedings of the IEEE/CVF Conference on Computer Vision and Pattern Recognition*. pp. 3677–3686 (2020)
9. Fang, Y., Wang, W., Xie, B., Sun, Q., Wu, L., Wang, X., Huang, T., Wang, X., Cao, Y.: Eva: Exploring the limits of masked visual representation learning at scale. In: *Proceedings of the IEEE/CVF Conference on Computer Vision and Pattern Recognition*. pp. 19358–19369 (2023)
10. Ganin, Y., Ustinova, E., Ajakan, H., Germain, P., Larochelle, H., Laviolette, F., Marchand, M., Lempitsky, V.: Domain-adversarial training of neural networks. *JMLR* (2016)
11. Ghadiyaram, D., Bovik, A.C.: Massive online crowdsourced study of subjective and objective picture quality. *IEEE Transactions on Image Processing* **25**(1), 372–387 (2015)
12. Ghildyal, A., Liu, F.: Shift-tolerant perceptual similarity metric. In: *European Conference on Computer Vision* (2022)

13. Gravitass, S.: Auto-gpt (2023), <https://github.com/Significant-Gravitas/Auto-GPT#auto-gpt-an-autonomous-gpt-4-experiment>
14. Hosu, V., Lin, H., Sziranyi, T., Saupé, D.: Koniq-10k: An ecologically valid database for deep learning of blind image quality assessment. *IEEE Transactions on Image Processing* **29**, 4041–4056 (2020)
15. Hu, E.J., Shen, Y., Wallis, P., Allen-Zhu, Z., Li, Y., Wang, S., Wang, L., Chen, W.: LoRA: Low-rank adaptation of large language models. In: *ICLR* (2022)
16. Ke, J., Wang, Q., Wang, Y., Milanfar, P., Yang, F.: Musiq: Multi-scale image quality transformer. In: *ICCV* (2021)
17. Koh, J.Y., Fried, D., Salakhutdinov, R.: Generating images with multimodal language models. *arXiv preprint arXiv:2305.17216* (2023)
18. Laurençon, H., Saulnier, L., Tronchon, L., Bekman, S., Singh, A., Lozhkov, A., Wang, T., Karamcheti, S., Rush, A.M., Kiela, D., et al.: Obelics: An open web-scale filtered dataset of interleaved image-text documents. In: *NeurIPS* (2023)
19. Li, B., Zhang, Y., Chen, L., Wang, J., Yang, J., Liu, Z.: Otter: A multi-modal model with in-context instruction tuning. *arXiv preprint arXiv:2305.03726* (2023)
20. Li, C., Zhang, Z., Wu, H., Sun, W., Min, X., Liu, X., Zhai, G., Lin, W.: Agiqa-3k: An open database for ai-generated image quality assessment. *arXiv preprint arXiv:2306.04717* (2023)
21. Li, D., Jiang, T., Jiang, M.: Unified quality assessment of in-the-wild videos with mixed datasets training. *International Journal of Computer Vision* **129**, 1238–1257 (2021)
22. Li, J., Li, D., Savarese, S., Hoi, S.: Blip-2: Bootstrapping language-image pre-training with frozen image encoders and large language models. *arXiv preprint arXiv:2301.12597* (2023)
23. Lin, H., Hosu, V., Saupé, D.: Kadid-10k: A large-scale artificially distorted iqa database. In: *2019 Eleventh International Conference on Quality of Multimedia Experience (QoMEX)*. pp. 1–3. *IEEE* (2019)
24. Lin, K., Yang, Z., Li, L., Wang, J., Wang, L.: Designbench: Exploring and benchmarking dall-e 3 for imagining visual design. *arXiv preprint arXiv:2310.15144* (2023)
25. Liu, H., Li, C., Wu, Q., Lee, Y.J.: Visual instruction tuning. *arXiv preprint arXiv:2304.08485* (2023)
26. Liu, J., Li, X., An, S., Chen, Z.: Source-free unsupervised domain adaptation for blind image quality assessment. *arXiv preprint arXiv:2207.08124* (2022)
27. Liu, X., Van De Weijer, J., Bagdanov, A.D.: Rankiqa: Learning from rankings for no-reference image quality assessment. In: *ICCV* (2017)
28. Loshchilov, I., Hutter, F.: Sgdr: Stochastic gradient descent with warm restarts. *arXiv preprint arXiv:1608.03983* (2016)
29. Loshchilov, I., Hutter, F.: Decoupled weight decay regularization. *arXiv preprint arXiv:1711.05101* (2017)
30. Lv, T., Huang, Y., Chen, J., Cui, L., Ma, S., Chang, Y., Huang, S., Wang, W., Dong, L., Luo, W., et al.: Kosmos-2.5: A multimodal literate model. *arXiv preprint arXiv:2309.11419* (2023)
31. Madhusudana, P.C., Birkbeck, N., Wang, Y., Adsumilli, B., Bovik, A.C.: Image quality assessment using contrastive learning. *IEEE Transactions on Image Processing* (2022)
32. Mangrulkar, S., Gugger, S., Debut, L., Belkada, Y., Paul, S.: Peft: State-of-the-art parameter-efficient fine-tuning methods. <https://github.com/huggingface/peft> (2022)

33. Mittal, A., Moorthy, A.K., Bovik, A.C.: No-reference image quality assessment in the spatial domain. *IEEE Transactions on image processing* (2012)
34. OpenAI: Gpt-4 (2023), <https://openai.com/research/gpt-4>
35. OpenAI: Gpt-4v(ision) system card (2023), https://cdn.openai.com/papers/GPTV_System_Card.pdf
36. Pan, X., Dong, L., Huang, S., Peng, Z., Chen, W., Wei, F.: Kosmos-g: Generating images in context with multimodal large language models. *arXiv preprint arXiv:2310.02992* (2023)
37. Pan, Z., Yuan, F., Lei, J., Fang, Y., Shao, X., Kwong, S.: Vcnet: Visual compensation restoration network for no-reference image quality assessment. *TIP* (2022)
38. Peng, Z., Wang, W., Dong, L., Hao, Y., Huang, S., Ma, S., Wei, F.: Kosmos-2: Grounding multimodal large language models to the world. *arXiv preprint arXiv:2306.14824* (2023)
39. Radford, A., Kim, J.W., Hallacy, C., Ramesh, A., Goh, G., Agarwal, S., Sastry, G., Askell, A., Mishkin, P., Clark, J., et al.: Learning transferable visual models from natural language supervision. In: *ICML* (2021)
40. Rajbhandari, S., Ruwase, O., Rasley, J., Smith, S., He, Y.: Zero-infinity: Breaking the gpu memory wall for extreme scale deep learning. In: *Proceedings of the International Conference for High Performance Computing, Networking, Storage and Analysis*. pp. 1–14 (2021)
41. Rasley, J., Rajbhandari, S., Ruwase, O., He, Y.: Deepspeed: System optimizations enable training deep learning models with over 100 billion parameters. In: *Proceedings of the 26th ACM SIGKDD International Conference on Knowledge Discovery & Data Mining*. pp. 3505–3506 (2020)
42. reworkd.ai: Agentgpt (2023), <https://github.com/reworkd/AgentGPT>
43. Roy, S., Mitra, S., Biswas, S., Soundararajan, R.: Test time adaptation for blind image quality assessment. In: *Proceedings of the IEEE/CVF International Conference on Computer Vision*. pp. 16742–16751 (2023)
44. Saha, A., Mishra, S., Bovik, A.C.: Re-iqa: Unsupervised learning for image quality assessment in the wild. In: *Proceedings of the IEEE/CVF Conference on Computer Vision and Pattern Recognition*. pp. 5846–5855 (2023)
45. Shen, Y., Song, K., Tan, X., Li, D., Lu, W., Zhuang, Y.: Hugginggpt: Solving ai tasks with chatgpt and its friends in huggingface. *arXiv preprint arXiv:2303.17580* (2023)
46. Streijl, R.C., Winkler, S., Hands, D.S.: Mean opinion score (mos) revisited: methods and applications, limitations and alternatives. *Multimedia Systems* **22**(2), 213–227 (2016)
47. Su, S., Yan, Q., Zhu, Y., Zhang, C., Ge, X., Sun, J., Zhang, Y.: Blindly assess image quality in the wild guided by a self-adaptive hyper network. In: *CVPR* (2020)
48. Sun, S., Yu, T., Xu, J., Zhou, W., Chen, Z.: Graphiqa: Learning distortion graph representations for blind image quality assessment. *Trans. Multi.* (2023)
49. Thong, W., Pereira, J.C., Parisot, S., Leonardi, A., McDonagh, S.: Content-diverse comparisons improve iqa. In: *BMVC* (2022)
50. Wang, J., Chan, K.C., Loy, C.C.: Exploring clip for assessing the look and feel of images. In: *AAAI* (2023)
51. Wang, J., Duan, H., Liu, J., Chen, S., Min, X., Zhai, G.: Aigciqa2023: A large-scale image quality assessment database for ai generated images: from the perspectives of quality, authenticity and correspondence. *arXiv preprint arXiv:2307.00211* (2023)
52. Wang, Z., Bovik, A.C., Sheikh, H.R., Simoncelli, E.P.: Image quality assessment: from error visibility to structural similarity. *IEEE transactions on image processing* **13**(4), 600–612 (2004)

53. Wu, H., Zhang, Z., Zhang, E., Chen, C., Liao, L., Wang, A., Li, C., Sun, W., Yan, Q., Zhai, G., et al.: Q-bench: A benchmark for general-purpose foundation models on low-level vision. arXiv preprint arXiv:2309.14181 (2023)
54. Yang, Z., Li, L., Lin, K., Wang, J., Lin, C.C., Liu, Z., Wang, L.: The dawn of lmms: Preliminary explorations with gpt-4v (ision). arXiv preprint arXiv:2309.17421 **9** (2023)
55. Yang, Z., Li, L., Wang, J., Lin, K., Azarnasab, E., Ahmed, F., Liu, Z., Liu, C., Zeng, M., Wang, L.: Mm-react: Prompting chatgpt for multimodal reasoning and action. arXiv preprint arXiv:2303.11381 (2023)
56. Ye, P., Kumar, J., Kang, L., Doermann, D.: Unsupervised feature learning framework for no-reference image quality assessment. In: IEEE conference on computer vision and pattern recognition (2012)
57. Ye, Q., Xu, H., Xu, G., Ye, J., Yan, M., Zhou, Y., Wang, J., Hu, A., Shi, P., Shi, Y., et al.: mplug-owl: Modularization empowers large language models with multimodality. arXiv preprint arXiv:2304.14178 (2023)
58. Ying, Z., Niu, H., Gupta, P., Mahajan, D., Ghadiyaram, D., Bovik, A.: From patches to pictures (paq-2-piq): Mapping the perceptual space of picture quality. In: Proceedings of the IEEE/CVF Conference on Computer Vision and Pattern Recognition. pp. 3575–3585 (2020)
59. You, H., Zhang, H., Gan, Z., Du, X., Zhang, B., Wang, Z., Cao, L., Chang, S.F., Yang, Y.: Ferret: Refer and ground anything anywhere at any granularity. arXiv preprint arXiv:2310.07704 (2023)
60. Yu, L., Lezama, J., Gundavarapu, N.B., Versari, L., Sohn, K., Minnen, D., Cheng, Y., Gupta, A., Gu, X., Hauptmann, A.G., et al.: Language model beats diffusion—tokenizer is key to visual generation. arXiv preprint arXiv:2310.05737 (2023)
61. Yu, L., Shi, B., Pasunuru, R., Muller, B., Golovneva, O., Wang, T., Babu, A., Tang, B., Karrer, B., Sheynin, S., et al.: Scaling autoregressive multi-modal models: Pretraining and instruction tuning. arXiv preprint arXiv:2309.02591 (2023)
62. Zhang, L., Zhang, L., Bovik, A.C.: A feature-enriched completely blind image quality evaluator. IEEE Transactions on Image Processing (2015)
63. Zhang, P., Wang, X.D.B., Cao, Y., Xu, C., Ouyang, L., Zhao, Z., Ding, S., Zhang, S., Duan, H., Yan, H., et al.: Internlm-xcomposer: A vision-language large model for advanced text-image comprehension and composition. arXiv preprint arXiv:2309.15112 (2023)
64. Zhang, W., Ma, K., Yan, J., Deng, D., Wang, Z.: Blind image quality assessment using a deep bilinear convolutional neural network. IEEE Transactions on Circuits and Systems for Video Technology (2018)
65. Zhang, W., Zhai, G., Wei, Y., Yang, X., Ma, K.: Blind image quality assessment via vision-language correspondence: A multitask learning perspective. In: Proceedings of the IEEE/CVF Conference on Computer Vision and Pattern Recognition. pp. 14071–14081 (2023)
66. Zhang, Z., Zhang, X., Xie, W., Lu, Y.: Responsible task automation: Empowering large language models as responsible task automators. arXiv preprint arXiv:2306.01242 (2023)
67. Zhang, Z., Sun, W., Zhou, Y., Jia, J., Zhang, Z., Liu, J., Min, X., Zhai, G.: Subjective and objective quality assessment for in-the-wild computer graphics images. *Acm T Multim Comput* (2023)
68. Zhao, K., Yuan, K., Sun, M., Li, M., Wen, X.: Quality-aware pre-trained models for blind image quality assessment. In: Proceedings of the IEEE/CVF Conference on Computer Vision and Pattern Recognition. pp. 22302–22313 (2023)

69. Zheng, K., He, X., Wang, X.E.: Minigpt-5: Interleaved vision-and-language generation via generative vokens. arXiv preprint arXiv:2310.02239 (2023)
70. Zhu, D., Chen, J., Shen, X., Li, X., Elhoseiny, M.: Minigpt-4: Enhancing vision-language understanding with advanced large language models. arXiv preprint arXiv:2304.10592 (2023)
71. Zhu, H., Li, L., Wu, J., Dong, W., Shi, G.: Metaiqa: Deep meta-learning for no-reference image quality assessment. In: Proceedings of the IEEE/CVF Conference on Computer Vision and Pattern Recognition. pp. 14143–14152 (2020)

[Supplementary Material]

In this supplementary material, we detail the experiment setup in Sec. 6, including the detailed introduction of training datasets in Sec. 6.1, hyper-parameter configurations in Sec. 6.2, and more details about the adopted prompts for data construction in Sec. 6.3. We present more experiment results in Sec. 7, including more quantitative results in Sec. 7.1 and more qualitative results in Sec. 7.2. Additionally, we present more discussion about the potential negative impact, limitations, and code release in Sec. 8.

6 More Details about Experiment Setup**6.1 Detailed Introduction of the Datasets**

In our main paper, we list all used datasets in Table 1. Aside from LLaVA-Instruction [25] and CCSBU-Aligned [70] which are used for instruction tuning, the data for visual quality learning is multi-sourced. Among these datasets, KonIQ-10k [14], SPAQ [8], FLIVE [58], LIVEC [11] comprise photographic images with in-the-wild distortions. KADID-10k [23] provide photographic images with artificial distortions. CGIQA-6K [67], AGIQA-3k [20] and AIGCIQA-2023 [51] are all AI-generated images. More details about each one can be found in their corresponding publications. Owing to the substantial diversity over these datasets, the annotation inconformity introduced in our main paper is extremely pronounced, imposing a big challenge in the joint training across them. For all datasets, except the artificially distorted KADID-10k [23], we randomly sample 80% of images as the training split while the remaining 20% as the test split. The KADID-10k contains about 10k images, derived from 81 pristine images. Each image is degraded by 25 distortions in 5 levels. To ensure the diversity between training and test sets, we adopt all the distorted images corresponding to 65 of the pristine images as the training set, while the distorted images corresponding to the remaining 16 pristine images are used as the test set. Each training pair in Stage-1 is randomly sampled from the same dataset. Its detailed formulation is in Sec. 3.2 of the main paper and the specific prompts for its construction are in Figure 3 of the main paper.

6.2 Hyper-parameter Configurations

We train VisualCritic with Zero-2 powered by deepspeed framework [40, 41]. The vision backbone has 1B parameters, and the vicuna model we used has 13B parameters, wherein the trainable parameters is 1B. The model is trained using a resolution of 224×224 at all stages. We employ the AdamW [29] optimizer paired with a cosine learning rate scheduler [28] for model training. In the first stage, we conduct the training for 100,000 steps on $4 \times A100$ GPUs, with a global batch size of 96 and a base learning rate of $2e-3$. This stage is completed in approximately 30 hours. In the second stage, the model is trained for 20,000 steps on $4 \times A100$ GPUs, maintaining a global batch size of 96 and a base learning rate of $2e-4$,

taking around 6 hours. Finally, the model undergoes an additional 5,000 training steps on 4×A100 GPUs, with a global batch size of 64, completed in about 1.5 hours. The maximum learning rate remains constant at 2e-5 during this final stage. We provide more detailed hyperparameter configurations in Table 8.

Table 8: Details of the hyperparameter configurations.

Training Configuration	Stage1	Stage2	Stage3
Base LR	0.001	0.0001	0.00008
Min. LR	0.0001	0.00001	0.000008
Warmup LR	0.00001	0.00001	0.000001
Warm-up scheduler	Linear	Linear	Linear
Scheduler	Cosine	Cosine	Cosine
Weight decay	0.01	0.05	0.05
Training iterations	50000	150000	10000
Warmup iterations	5000	10000	1000
LoRA_r	16	16	16
LoRA_alpha	32	32	32
LoRA_dropout	0.1	0.1	0.1
Batch size	128	64	64
Iteration	100000	50000	8000
Training Time	20 h	10 h	1.6 h

6.3 Prompts for Data Construction

As introduced in our main paper, the training data for enabling different assessment functionalities share a unified data format as below, where $\{img_content\}$, $\{instruction_content\}$ and $\{answer_content\}$ are three placeholders of the tokens of input image, user instruction and VisualCritic’s response, respectively.

Human: < $img1$ > $\{img1_content\}$ < / $img1$ > (< $img2$ > $\{img2_content\}$ < / $img2$ >)[$Task$
Identifier] $\{instruction_content\}$
Assistant: $\{answer_content\}$

The prompts to generate $\{answer_content\}$ are illustrated in Figure 3 in the main paper. The prompt generating user instruction (*i.e.*, $\{instruction_content\}$) are shown in Figure 4.

7 More Experiment Results

7.1 More Quantitative Results

Within-dataset comparison with IQA specialist models. We have demonstrated the unprecedented generalizability of our proposed VisualCritic in Ta-

You are an AI data construction assistant. I will provide the name of a visual quality metric. You need to return me an instruction query for it accordingly.

EXAMPLE 1:

=====

INPUT: MOS

OUTPUT:

How would you rate the Mean Opinion Score (MOS) of this image?

EXAMPLE 2:

=====

INPUT: Brightness

OUTPUT:

Can you estimate the brightness level of this picture?

Fig. 4: LLM prompts for data construction, *i.e.*, generating the $\{instruction_content\}$ in the training data.

ble 3 of our main paper. Here, we further compare VisualCritic to the state-of-the-art IQA specialist models in terms of their within-dataset quantitative performance. As shown in Table 9, our proposed VisualCritic delivers comparable within-dataset performance with those conventional IQA models, and even outperforms some of them. This is actually not easy since our VisualCritic is trained on diverse data with the aforementioned annotation inconformity issue over both photographic and AI-generated images. As a common sense in the IQA field, these conventional models, trained on an individual dataset, can easily fit one particular dataset but struggle to generalize to other datasets right out of box. Note that the generalizability and versatility are the primary exploration objectives of this paper, while the within-domain performance is not. We thus place these results in the supplementary material and leave the improvements in the balance of within-dataset and cross-dataset performance in our future studies.

Table 9: Comparison results (MOS) of our VisualCritic with the state-of-the-art IQA specialist models for within-dataset settings.

Dataset	KonIQ-10k	SPAQ	LIVEC	KADID10k	FLIVE	
BRISQUE [33]	0.665/0.681	0.809/0.817	0.608/0.629	0.528/0.567	0.288/0.373	
CORNIA [56]	0.780/0.795	0.709/0.725	0.629/0.671	0.516/0.558	-	
ILNIQE [62]	0.507/0.523	-	0.432/0.508	-	-	
DBCNN [64]	0.875/0.884	0.911/0.915	0.851/0.869	0.851/0.856	0.580/0.641	
CONTRIQUE [31]	0.894/0.906	0.914/0.919	0.845/0.857	0.934/0.937	0.580/0.641	
MUSIQ [16]	0.916/0.928	0.917/0.921	-	-	0.646/0.739	
Re-IQA [44]	0.914	0.923	0.918/0.925	0.840/0.854	0.872/0.885	0.645/0.733
VisualCritic	0.856/0.867	0.865/0.864	0.857/0.864	0.855/0.843	0.633/0.667	

The accuracy of relativity learning. As introduced in Sec 3.2 and Table 5 in the main paper, relativity learning is an important part of our VisualCritic, we show the accuracy of this in Table 10. As the results shown, judging a pair with ranking is slightly better than directly doing A-B on their scores.

Combining 2 or 3 training datasets. As illustrated in Table 3 of the main paper, $MultiFunc_{single}$ significantly outperforms $MultiFunc_{joint}$. This demon-

Table 10: Comparison the accuracy of relativity learning with directly doing A-B on their output scores.

Methods	KonIQ	SPAQ	FLIVE	LIVEC	CGIQA	KADID	AGIQA
Ranking	0.85	0.86	0.76	0.80	0.74	0.79	0.82
A-B scores	0.81	0.84	0.72	0.76	0.70	0.77	0.80

strates the existence of the aforementioned annotation inconformity issue and presents a solution. While there are alternative approaches, such as combining two or three datasets instead of all seven, these methods do not fundamentally differ from using all seven datasets (*MultiFunc_{joint}*) because they still encounter the annotation inconformity issue. Furthermore, exhaustively training on all 127 combinations from the sum $\sum_{k=1}^7 C(7, k)$ to seek the highest performing structure is not only impractical due to the computational resources required, but it also falls outside the scope of this paper. We have provided a comparison with combinations of two or three datasets in Table 11 for reference. Our experimental results have not shown any performance improvements over experiments conducted with single training datasets.

Table 11: Comparison of models trained with combinations of two and three datasets versus models trained with single datasets in the Stage-2. ‘Two’ denotes ‘KonIQ+FLIVE’, ‘Three’ represents ‘KonIQ+SPAQ+CGIQA’ and ‘Single’ means ‘KonIQ’.

Datasets.	KonIQ	SPAQ	FLIVE	LIVEC	CGIQA	KADID	AGIQA
Two	0.722/0.741	0.766/0.789	0.467/0.485	0.638/0.664	0.334/0.357	0.507/0.521	0.644/0.668
Three	0.694/0.733	0.723/0.736	0.288/0.314	0.553/0.579	0.294/0.301	0.443/0.496	0.584/0.563
Single	0.856/0.867	0.844/0.852	0.553/0.633	0.738/0.778	0.442/0.473	0.681/0.701	0.734/0.712

7.2 More Qualitative Results

More results on qualitative evaluation We have illustrated the comparison results between VisualCritic and other LMMs regarding qualitatively commenting on the visual quality of a given image in our main paper. Here, we present more in Figure 5. In this regard, MiniGPT-4 [70] seems to have a bias of considering all images as the ones with high visual quality. LLaVA [25] and InstructBLIP [7] often provide responses that are irrelevant to the instructions, that is, their responses do not contain any content related to visual quality. GPT-4V [54] can give basically reasonable answers in this regard but performs poorly in quantitative measurement and authenticity detection. They all include the contents related to semantic understanding in their responses, while our VisualCritic is more focused on the visual quality in line with the instructions.

More results on authenticity detection We present more results on the case studies regarding authenticity detection in Figure 6. As shown in this figure, the

 <p>Ground-truth: MOS: 25.17 Brightness: 35.00 Colorfulness: 34.67 Contrast: 32.50 Noisiness: 32.00 Sharpness: 17.17</p>	<p> User Instruction: <IQA_DES> Please describe in words the visual quality of this image.</p> <p># MiniGPT-4: The image shows a group of people standing near a small red car that is parked on the sidewalk. The car appears to be damaged and has a broken window on the driver's side. There is a green metal fence in the background and a few trees on the sidewalk. The sky is dark and there are some streetlights on the street. The image is well-lit and the colors are vibrant. The overall visual quality of the image is clear and well-composed.</p> <p># LLaVA: The image is a black and white photograph of a small tractor or truck parked on a sidewalk. There are two people standing near the vehicle, one on the left side and the other on the right side. The scene appears to be set at night, as the surroundings are dark, and the vehicle is parked on the side of the road. The presence of the people suggests that they might be the owners or passengers of the vehicle. (Failed to describe the visual quality of the image)</p> <p># InstructBLIP: The image features a street scene at night, with people walking along the sidewalk next to a red tricycle. There is also a small group of people standing in front of a brick wall and a sign that reads "No Parking" on the side of the road. (Failed to describe the visual quality of the image)</p> <p># GPT-4V: The image you've uploaded appears to be of low to moderate visual quality. It seems to be taken during evening or night-time, given the artificial lighting and the darkness of the sky. The photo is a bit blurry, which suggests either a low-resolution camera was used or the camera moved during the shot. The focus is not sharp, and details are not crisp, which affects the ability to discern finer details. There is visible noise or grain, likely due to the low light conditions, which is common in photos taken with a high ISO setting or a less capable camera in dim lighting. The composition of the image is somewhat cluttered, with multiple elements such as people and objects in the frame. The lighting conditions, with a mix of shadows and artificial light, add to the visual noise of the photo.</p> <p># VisualCritic (Ours): The image has been assessed across various visual quality parameters, its overall mean opinion score MOS indicates a relatively low subjective quality perception, the image exhibits a somewhat dim brightness level, which might make it difficult to discern certain details, the colors present are somewhat dull, lacking vibrancy and liveliness, the contrast between lighter and darker areas is limited, which may affect the visual depth and clarity, a considerable amount of noise can be observed, possibly due to graininess or other artifacts, which could be distracting, the details in the image are not very clear, and there is significant room for improvement in terms of sharpness and crispness.</p>
 <p>Ground-truth: MOS: 26.63 Brightness: 48.25 Colorfulness: 59.71 Contrast: 47.29 Noisiness: 39.88 Sharpness: 17.38</p>	<p> User Instruction: <IQA_DES> Please describe in words the visual quality of this image.</p> <p># MiniGPT-4: The image shows a row of bicycles parked on the sidewalk in front of a building with tall trees in the background. The image details are clear.</p> <p># LLaVA: The image is a black and white photo of a city street with a row of parked cars on the side of the road. There are several bicycles parked in a line, with some of them being yellow. The scene also features a few motorcycles parked among the bicycles. The street is lined with trees, adding a touch of greenery to the urban environment. The overall atmosphere of the image is nostalgic and reminiscent of a bygone era.</p> <p># InstructBLIP: There are several bicycles parked next to each other on the sidewalk in front of a building with tall buildings in the background. It is likely that there are multiple people using these bikes at the same time. (Failed to describe the visual quality of the image)</p> <p># GPT-4V: The image you've uploaded is significantly blurred, resulting in a lack of sharpness and detail across the entire scene. There's a complete absence of clear edges or fine detail, which suggests that the camera was out of focus when the picture was taken or there was movement during the exposure. The colors and shapes are smeared, and it's difficult to identify specific objects or features with any clarity. This level of blur affects the image's usefulness for identifying details or subjects within the scene.</p> <p># VisualCritic (Ours): The image has been assessed across various visual quality parameters, its overall mean opinion score MOS indicates a somewhat low subjective quality perception, the image exhibits a fairly balanced brightness level, ensuring it's neither too dark nor excessively bright, the colors present are moderately vibrant, contributing to a lively visual experience, the contrast between lighter and darker areas is average, providing a decent sense of visual depth and clarity, however, there is a significant amount of noise present, which could be due to graininess or other artifacts, the details in the image are not very clear, and there is considerable room for improvement in terms of sharpness and crispness.</p>
 <p>Ground-truth: MOS: 73.08 Brightness: 69.25 Colorfulness: 80.92 Contrast: 74.69 Noisiness: 76.75 Sharpness: 75.92</p>	<p> User Instruction: <IQA_DES> Please describe in words the visual quality of this image.</p> <p># MiniGPT-4: The image is a view of a park with a lamppost in the foreground and a row of trees in the background. The sky is cloudy and there are some buildings visible in the distance. The image is fairly clear and the colors are muted. The lighting is fairly bright, with the sun shining down on the scene. The overall visual quality of the image is fairly good.</p> <p># LLaVA: The image features a cityscape with a large tree in the foreground, surrounded by a grassy area. The tree is bare, indicating that it is likely during the winter season. In the background, there are several tall buildings, creating a contrast between the natural tree and the urban environment. The scene is captured on a cloudy day, which adds a moody atmosphere to the image. (Failed to describe the visual quality of the image)</p> <p># InstructBLIP: The image features a green park with a tree and a lamppost in the background. There is a lake near the park, as well as several buildings in the distance. It appears to be a cloudy day. (Failed to describe the visual quality of the image)</p> <p># GPT-4V: The image appears to be of a park or a natural area with a view towards a body of water and buildings in the background. The visual quality is clear with no apparent blur, allowing for distinct edges and details to be visible. The lighting seems to be overcast, with no harsh shadows, which provides even illumination across the scene. The colors are somewhat muted, which could be due to the lighting conditions or the settings of the camera. There is a good contrast between the trees, the lamp post, and the sky, and the composition is balanced with natural elements in the foreground and urban structures in the distance. Overall, the image is well-composed and of good visual quality.</p> <p># VisualCritic (Ours): The image has been assessed across various visual quality parameters, and the overall mean opinion score MOS indicates a high level of subjective quality perception. The image exhibits an optimal brightness level, ensuring a comfortable viewing experience. The colors are vivid and lively, contributing to an engaging visual presentation. The contrast is excellent, providing a clear distinction between lighter and darker areas, which enhances the overall depth and clarity. The image has minimal noise, resulting in a clean and smooth appearance. The sharpness is outstanding, showcasing a high level of detail and crispness throughout the image.</p>

Fig. 5: More comparison results between our VisualCritic and other LMMs on qualitative evaluation. Errors are red-highlighted.

open-source LMMs MiniGPT-4 [70], LLaVA [25] and InstructBLIP [7] all tend to regard the given images as real/photographic, whether these images are actually real or AI-generated. Our proposed VisualCritic provides the most accurate judgements, aligned with the ground-truths. Besides, the degree of certainty for these judgements can also be reflected in their responses.

Answers with unknown or uncertain judgements Besides our targeted generalizability and versatility, we also make additional efforts in minimizing







 <p>Ground-truth Authenticity: 35.43</p>	<p> User Instruction: <IQA_AUTH> Is it a real photo or an AI-generated image?</p> <p># MiniGPT-4: This image appears to be a real photo of a slice of green cucumber on a wooden surface. The cucumber is cut in half, with the seed and skin visible on the left side and the flesh on the right side. The surface of the cucumber is rough and textured, with small bumps and ridges visible. The lighting in the image is bright and even, with no shadows or highlights. The color of the cucumber is a bright green, with no other colors visible in the image. The overall mood of the image is natural and fresh.</p> <p># LLaVA: It is real image of a green pepper.</p> <p># InstructBLIP: The image is a real photo that was taken by a professional photographer.</p> <p># GPT-4V: If you notice any such inconsistencies, it could be AI-generated. Conversely, if the imperfections and details align with what's expected from real-world physics and optics, it's more likely to be a photograph. In the absence of distinctive markers for AI generation, it would be prudent to assume that the image is a real photograph. However, without further analysis and more information about the source and context of the image, it is not possible to provide a definitive answer.</p> <p># VisualCritic (Ours): This image strongly seems to be an AI-generated image.</p>
 <p>Ground-truth Authenticity: 46.83</p>	<p> User Instruction: <IQA_AUTH> Is it a real photo or an AI-generated image?</p> <p># MiniGPT-4: The image appears to be a real photo of a group of dogs in a city street. The dogs are all different breeds and sizes, and they are all walking together in a line. There are people in the background, but they are not interacting with the dogs. The image appears to be taken in a busy city street with a lot of people and buildings in the background.</p> <p># LLaVA: The image is a real photo of a dog parade in New York City..</p> <p># InstructBLIP: The image is a real photo taken by a professional photographer.</p> <p># GPT-4V: The image you've uploaded, which appears to show a large number of dogs of various breeds congregating in an urban environment like Times Square, has several indicators that suggest it is not a typical real-life photograph: The repetition of certain dogs in the same stance or position is not something that usually happens in spontaneous photography. The scene itself is highly unusual, as one would not typically see such a large number of dogs behaving in this organized manner without any human presence or leashes. These factors combined suggest that the image is likely digitally altered or AI-generated.</p> <p># VisualCritic (Ours): This image could be an AI-generated image.</p>
 <p>Ground-truth Authenticity: 100</p>	<p> User Instruction: <IQA_AUTH> Is it real photo or an AI-generated image?</p> <p># MiniGPT-4: The image is an AI-generated image. It shows a body of water with some green plants growing on the banks. There is a building in the background with white windows and a blue roof. The sky is cloudy and there are some white clouds in it.</p> <p># LLaVA: It is a real photo of a tree with yellow flowers and a body of water.</p> <p># InstructBLIP: The image is a real photo taken by a professional photographer.</p> <p># GPT-4: The image you have uploaded appears to be a real photograph. It displays characteristics typically associated with photos taken by digital cameras or smartphones, such as: Natural variation in lighting and shadows. Authentic looking textures on the trees, building, and surface of the water. Realistic color gradients in the sky and reflections in the water. An organic distribution of elements like the yellow flowers, which show natural growth patterns rather than repeated, patterned placement that might indicate digital generation.</p> <p># VisualCritic (Ours): This image looks like a real photo.</p>

Fig. 6: More comparison results between our VisualCritic and other LMMs on authenticity detection. Errors are red-highlighted.

the generation of hallucinations and actively admits its unknown or uncertain judgments. To achieve this, we add extra carefully designed training samples to enable VisualCritic to inform users when user instructions are out of the range that its knowledge currently covers. We showcase the performance of VisualCritic in this kind of scenarios in Figure 7. Please note that this is an additional point we consider for building a practical system, not as the focus of this research paper.

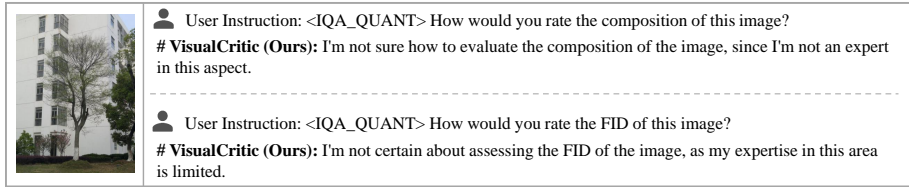


Fig. 7: Illustration of the answers given by our proposed VisualCritic with unknown or uncertain judgements.

8 More discussion

Potential negative impact. Job displacement may arise as automated assessments reduce the demand for human expertise in visual assessment industries. Additionally, overreliance on the LVLM for image quality assessments may lead to a devaluation of human judgment, risking the neglect of nuanced analysis that AI cannot replicate.

Limitation. The limitation mainly lies in that all training data of this work come from existing IQA datasets. Collecting more high-quality labeled data and extending this work to other types of data (*e.g.*, audio, 3D data, *etc.*), while beyond the current research scope, is very worthwhile to pursue in the future.

Code release. Our data, code, and models will be released upon paper acceptance.